IGF-1C Modified Hydrogel Enhances Cell Therapy for Acute Kidney Injury

Guowei Feng, Jimin Zhang, Yang Li, Yan Nie, Dashuai Zhu, Ran Wang, Jianfeng Liu, Jie Gao, Na Liu, Ningning He, Wei Du, Hongyan Tao, Yongzhe Che, Yong Xu, Deling Kong, Qiang Zhao, Zongjin Li

Supplemental Methods

Differentiation potential assay. To assess the multi-differentiation capacity of ADSCs, cells were cultured in adipogenic, osteogenic, and chondrogenic medium according to the manufacturer's instructions (Invitrogen). Adipogenic and osteogenic differentiation was performed by incubation in induction medium for 14 days (replaced every 2-3 days). Oil red O staining (Sigma-Aldrich) was used to assess the presence of intracellular lipid vacuoles. Alizarin red S (Sigma-Aldrich) was used to detect calcium deposits. Chondrogenesis was evaluated in ADSCs centrifuged to form a pellet and cultured in induction medium for 3-4 weeks. Cell clump was fixed in paraformaldehyde and stained with toluidine blue to detect proteoglycans. In order to evaluate the effect of exposure to hydrogel on cell multipotency, ADSCs were cultured on chitosan or CS-IGF-1C hydrogel coated plates for 1 or 2 weeks prior to induction.

Quantitative RT PCR. In order to evaluate the proliferation and apoptosis-related gene expression of ADSCs *in vitro* culture, cells were pre-treated with chitosan or CS-IGF-1C hydrogel for 2 weeks prior to RNA isolation. Besides, renal tissues were harvested to appraise the expression of apoptosis-related genes at 2 months. Total RNA was isolated from the cells or kidneys by TRIzol reagent (Invitrogen, Grand Island, NY) according to the manufacturer's directions. First-strand cDNA was synthesized using oligo dT primers with reverse transcriptase

(TransGen Biotech, China). Subsequently, real-time RT-PCR was performed on Opticon® System (Bio-Rad, Hercules, CA) in 20 μl reaction volumes. The mRNA expression levels were quantified using TransStart Green qPCR SuperMix Kit (TransGen Biotech, China). The $2^{-\Delta\Delta}$Ct method was used to determine the relative mRNA folding changes. Primers are listed in **Supplemental Table 1**.

Histological analysis. At indicated time points, mice were sacrificed and kidney samples were collected and fixed. Paraffin sections (5 μm) were stained with periodic acid-Schiff (PAS) (day 3), and Masson's trichrome (day 60). Histologic assessment of tubular injury was determined semiquantitatively using a method modified from a previous report[1]. Sections were scored independently by two investigators who were blinded to the treatment of the animal. In each sample, at least 100 proximal tubules were scored. The percentage of fibrosis was estimated by trichrome-stained surface compared to total kidney tissue area (n = 5 per group). Additionally, kidney sections of 2 months were stained with oil red O, alizarin red S, and toluidine blue to detect the ectopic differentiation in long term.

For immunofluorescent staining, animals were euthanized and the kidneys were perfused. All kidney specimens were embedded in paraffin or OCT compound (Miles Scientific), then sectioned to 5 μm slides and processed for immunostaining. Monoclonal rabbit anti-mouse PCNA (Abcam, Cambridge, MA) and Ki-67 (Boster, China) were used assessing cell proliferation at day 3 after AKI. TUNEL assay was performed at day 3 to evaluate apoptotic cell death using DeadEnd Fluorometric TUNEL System (Promega, Madison, WI) according to the manufacturer's directions. For angiogenesis analysis, sections were stained on 3 and 14 days

using CD31 (rat anti mouse, BD, San Jose, CA). To determine renal fibrosis, 2-month kidney sections were incubated with monoclonal rat anti-mouse Collagen IV (Abcam, Cambridge, MA), MMP2 (Abcam, Cambridge, MA). Alexa Fluor 594- and 488-conjugated secondary antibodies (Invitrogen, Grand Island, NY) were applied appropriately. Rhodamine/Fluorescein/DyLight 649-labeled lens culinaris agglutinin (LCA, Vector Laboratories) were used to stain proximal tubules. DAPI was used for nuclear counterstaining. For quantification, 12 microscopic fields (magnification, 200 or 400) of four samples obtained from each animal (n=5 per group) were analyzed. The number of positively stained cells was counted by a blinded investigator.

Supplemental Results

Characterization of ADSCs. In our study, ADSCs were isolated from transgenic mice that constituently express firefly luciferase (Fluc) and green fluorescent protein (GFP). These cells exhibited strong proliferative capacity in *in vitro* culture (**Supplemental Figure 2A**). Immunofluorescent observation and flow cytometry analysis confirmed the robust expression of GFP in ADSCs (**Supplemental Figure 2B&C**). In addition, bioluminescence imaging revealed a linear correlation between cell number and Fluc reporter gene activity, indicating the transgenic properties of ADSCs (**Supplemental Figure 2D&E**).

Biocompatibility of CS-IGF-1C hydrogel. The CS-IGF-1C hydrogel used in this study has an IGF-1C concentration around 2.0 mg/ml [2.0‰ (w/v)], which showed excellent biocompatibility and bioactivity in our pilot study. To examine the biocompatibility of the hydrogels, ADSCs were cultured on non-coated, chitosan or CS-IGF-1C hydrogel coated plates. CS-IGF-1C hydrogel enhanced the colony-forming capacity of ADSCs when compared to the other

conditions (**Supplemental Figure 3A**). In addition, live/dead assay was conducted to assess cytocompatibility of chitosan hydrogel and CS-IGF-1C hydrogel by culturing cells for prolonged period, revealing both hydrogels are not toxic to ADSCs (**Supplemental Figure 3B&C**). This pro-mitogenic effect was consolidated by CCK-8 assay (**Supplemental Figure 3D**).

Influence of hydrogels on phenotype and multipotency of ADSCs. Next, we determined if *in vitro* exposure to hydrogel could affect the phenotypic characteristic and differentiation capacity of ADSCs. After a 2-week culture on chitosan or CS-IGF-1C hydrogel coated plates, ADSCs maintained the expression of surface markers (CD29, CD44, CD73, CD90, and CD105) typically found on MSCs (**Supplemental Figure 4A**). Meanwhile, they consistently lack endothelial and hematopoietic markers (CD31, CD34, and CD45). Besides, after 2-week exposure to hydrogels, ADSCs were still capable of differentiating into cells of mesodermal lineage, including adipocytes, osteocytes, and chondrocytes (**Supplemental Figure 4B**). These results indicate that the phenotypic and multidifferentiation properties of ADSCs were not influenced by CS-IGF-1C or chitosan hydrogel in *in vitro* culture.

CS-IGF-1C hydrogel strengthens the anti-inflammatory effects of ADSCs. To explore if CS-IGF-1C hydrogel impacts immunoregulatory action of ADSCs, we measured the expression of inflammation-related genes in renal tissue 3 days after injury. ADSCs delivered by CS-IGF-1C hydrogel markedly down-regulated renal expression of pro-inflammatory (TNF-α, MCP-1, M-CSF, and RANTES) genes (**Supplemental Figure 5A**), whereas up-regulated anti-inflammatory (IL-10 and eNOS) and anti-oxidative (NQO-1 and glutathione peroxidase-1) genes (**Supplemental Figure 5B**) compared with the other treatment groups. These data reveal that

CS-IGF-1C hydrogel could enhance anti-inflammatory and anti-oxidative actions of ADSCs in AKI model.

CS-IGF-1C hydrogel facilitates cell proliferation. In order to elucidate the long-term effect of CS-IGF-1C hydrogel on cell proliferation, we evaluated the number of $PCNA^+$ cells within hydrogel injection sites and border zone at 28 days. $PCNA^+$ cells were rarely seen in chitosan hydrogel injection position (**Supplemental Figure 7A**). More $PCNA^+$ cells were detected within injection sites of ADSCs co-transplanted with CS-IGF-1C hydrogel group than those of chitosan hydrogel group (**Supplemental Figure 7B**). Consistent results were observed when assessing proliferative cells in regions of border zone to hydrogel injection sites (**Supplemental Figure 7C**).

Recovery of renal function after AKI. Next, we performed immunostaining to investigate the underlying mechanisms by which CS-IGF-1C hydrogel enhanced the anti-fibrotic action of ADSCs. Differentiated myofibroblasts, identified as α-smooth muscle actin (α-SMA) cells, are the primary cells that produce ECM during kidney fibrosis. Consistent with the results of collagen deposition, ADSCs and CS-IGF-1C co-transplantation therapy resulted in the most significant reduction of the number of $\alpha\text{-SMA}^+$ cells (**Supplemental Figure 8, A and B**). Moreover, matrix metalloproteinase 2 (MMP-2) is a principal mediator of ECM degradation, and its overexpression in transgenic mice promotes renal fibrosis[2]. Treatment with chitosan hydrogel or ADSCs attenuated the increased expression of MMP-2, which was further decreased in ADSCs and CS-IGF-1C hydrogel co-transplantation group (**Supplemental Figure 8, C and D**).

Maldifferentiation of ADSCs delivered by hydrogel. Despite their therapeutic benefits, MSCs were reported to maldifferentiate into glomerular adipocytes[3]. Thus, safety must be assured before further clinical translation. We performed oil red O, alizarin red S, and toluidine blue staining on 2-month kidney sections to assess whether administration of ADSCs leads to ectopic differentiation, i.e. adipogenesis, osteogenesis, and chondrogenesis, and to examine the possibility that the use of hydrogel could increase the risk of cell-induced maldifferentiation. No ectopic differentiation was observed in animals receiving any treatment modalities (**Supplemental Figure 9**), indicating the safety of our therapeutic approach.

Supplementary Table 1: Primers used for real-time RT-PCR

Transcription	Prime sequences
IGF-1	Forward: TGGATGCTCTTCAGTTCGTG
	Reverse: GTCTTGGGCATGTCAGTGTG
HGF	Forward: GAACTGCAAGCATGATGTGG
	Reverse: GATGCTGGAAATAGGGCAGAA
EGF	Forward: GAGCCACCCTCATAATCACA
	Reverse: CCCGAGTTCTTCTAAGTTCCT
Caspase-3	Forward: GGCACAAAGCGACTGGATG
	Reverse: CTGCCGTGGTACAGAACTGG
Caspase-9	Forward: ATCTGGCTCGGGGTTACTG
	Reverse: CTGCGTGGTGGTCATTCTC
Bax	Forward: TGAGCACTCCCGCCACAAA
	Reverse: CAGGATGCGTCCACCAAGAA
Bad	Forward: TGATGGCTGCTGCTGGTTG
	Reverse: CCCAGAGTTTGAGCCGAGTG
Fas	Forward: TGGAGGACAGGGCTTATGG
	Reverse: GCATCTGGACCCTCCTACCT
FasL	Forward: CCAGGCCCAATCCTACCAA
	Reverse: GCCCTCCAGGCACAGTTCTT
TNF-α	Forward: ACAGAAAGCATGATCCGCG
	Reverse: GCCCCCCATCTTTTGGG
MCP-1	Forward: CCACTCACCTGCTGCTACTCAT
	Reverse: TGGTGATCCTCTTGTAGCTCTCC
RANTES	Forward: CATATGGCTCGGACACCACT
	Reverse: ACACACTTGGCGGTTCCTTC
M-CSF	Forward: CATCCAGGCAGAGACTGACA
	Reverse: CTTGCTGATCCTCCTTCCAG
IL-10	Forward: TGAGGCGCTGTCGTCATCGATTTCTCCC
	Reverse: ACCTGCTCCACTGCCTTGCT
eNOS	Forward: GAAGGCTTTTGATCCCCGGGTCCTG
	Reverse: CAGTTCCTCCAGCCGTGTGTCCAC
NQO-1	Forward: TGGCCGAACACAAGAAGCTG
	Reverse: GCTACGAGCACTCTCTCAAACC
GSR-1	Forward: TTCGACGGGACCCAAA

	Reverse: ACATCGGGGTAAAGGC
Ang-1	Forward: ACAGGGACAGCAGGCAAAC
	Reverse: GGCATCGAACCACCAACC
Ang-2	Forward: GACTGGGAAGGCAACGAG
	Reverse: CTGAGAGCATCTGGGAACA
VEGF-A	Forward: ACTGGACCCTGGCTTTAC
	Reverse: TCTGCTCTCCTTCTGTCGTG
HIF-1α	Forward: GTGCACCCTAACAAGCCGGGG
	Reverse: AGCACCAAGCACGTCATGGGT
PLGF	Forward: CTTCTGAGTCGCTGTAGTGG
	Reverse: TCCTTTCTGCCTTTGTCG
PDGF-BB	Forward: ATCCAGGGAGCAGCGAGCCA
	Reverse: CAGGGCCGCCTTGTCATGGG
FGF-2	Forward: GCATCACCTCGCTTCCCGCA
	Reverse: CGCAGGAAGAAGCCGCCGTT
CCL5	Forward: TGCCCACGTCAAGGAGTATTTC
	Reverse: AACCCACTTCTTCTCTGGGTTG
Col1A1	Forward: ACTTCACTTCCTGCCTCAG
	Reverse: TGACTCAGGCTCTTGAGGGT
TGF-β	Forward: GTCAGACATTCGGGAAGCAG
	Reverse: GCGTATCAGTGGGGGTCA
Fibronectin	Forward: ATGTGGACCCCTCCTGATAGT
	Reverse: GCCCAGTGATTTCAGCAAAGG
MMP-9	Forward: GTCTTCCTGGGCAAGCAGTA
	Reverse: CTGGACAGAAACCCCACTTC
GAPDH	Forward: TTGTCTCCTGCGACTTCAAC
	Reverse: GTCATACCAGGAAATGAGCTTG

Supplemental Figures & Legends

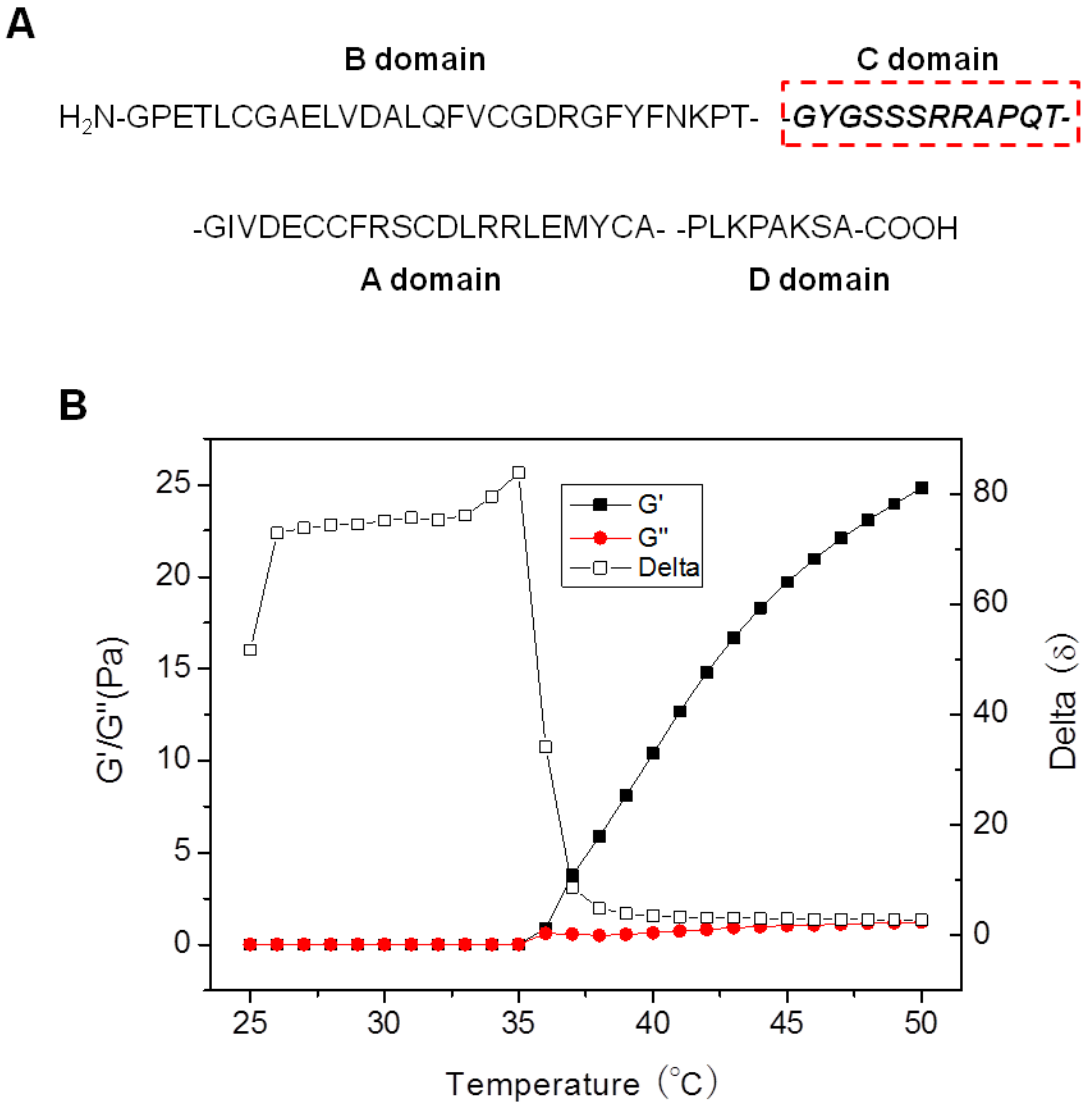

Supplemental Figure 1. (A)The amino acids sequence of IGF-1. IGF-1 protein comprises four domains. The C domain peptide was synthesized and utilized in this study. (**B**) **and rheological analysis of chitosan hydrogel with temperature changes**.

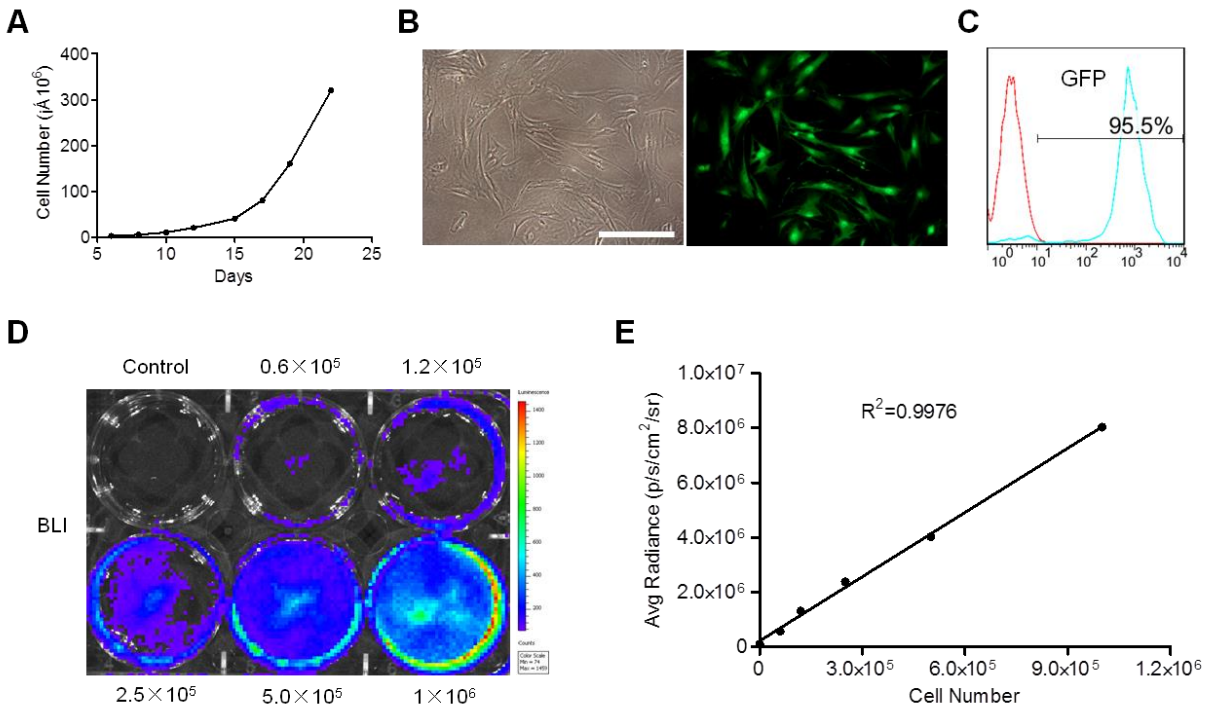

Supplemental Figure 2. Characterization of ADSCs isolated from transgenic mice. (**A**) The proliferative capacity of ADSCs in *in vitro* culture. (**B**) ADSCs were spindle-like in shape and GFP positive. (**C**) These cells exhibited robust expression of GFP as shown by flow cytometry. (**D-E**) BLI quantification demonstrated a robust linear correlation between the number of ADSCs and Fluc average radiance. Scale bar, 100 μm.

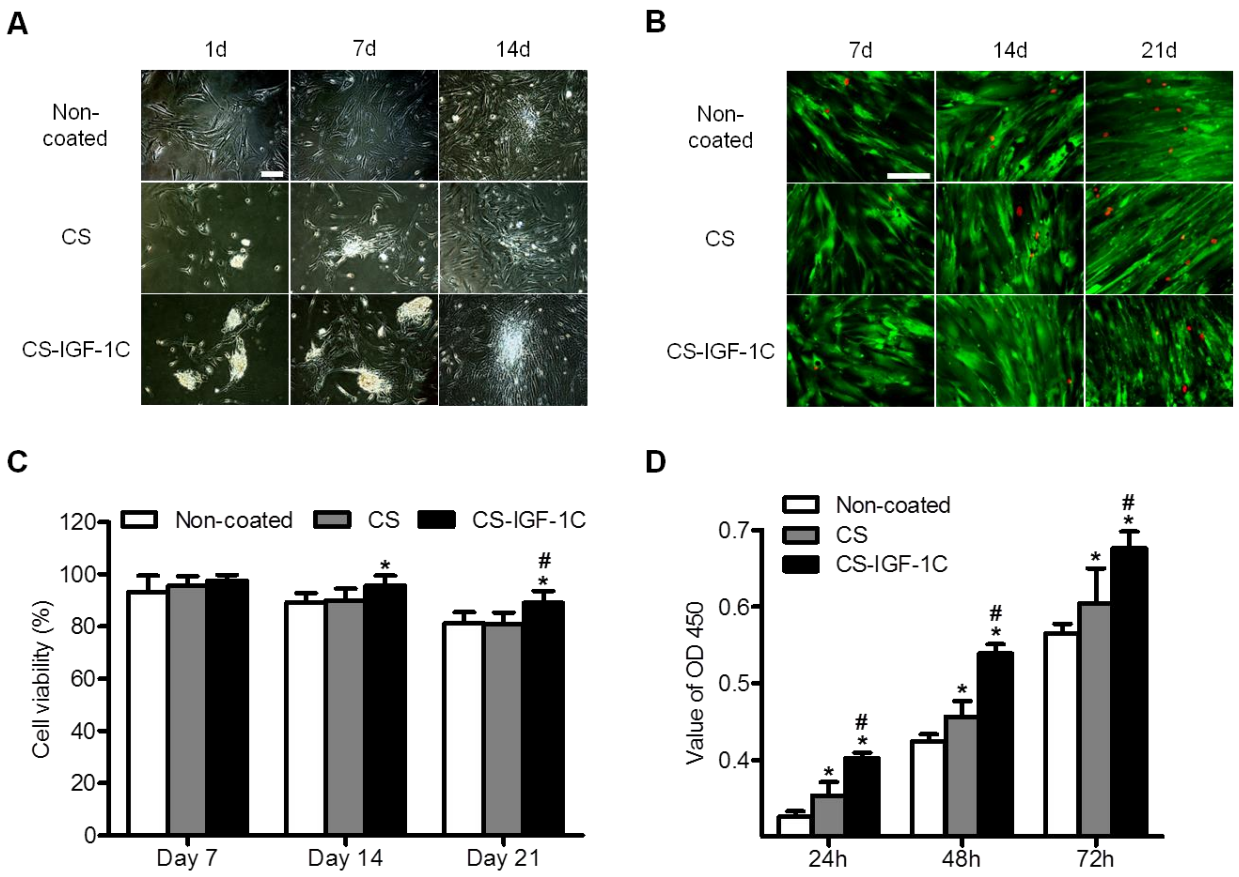

Supplemental Figure 3. Cell morphology and hydrogel biocompatibility. (**A**) The morphology and colony-forming capacity of ADSCs cultured on non-coated, CS, or CS-IGF-1C-coated plates for 1, 7, and 14 days. (**B**) Live/dead staining of GFP^+ ADSCs cultured on different conditions for 3 weeks. Red indicates dead cells. (**C**) Quantification of cell viability by calculating the percentage of live cells. n = 4. (**D**) CCK-8 assay revealing the proliferation of ADSCs cultured on different conditions for 3 days. n = 4. $^*P < 0.05$ vs CS, $^{\#}P < 0.05$ vs ADSCs/CS. The experiments of live/dead staining and CCK-8 assay were repeated for 3 times. Scale bars, 50 μm. CS, chitosan hydrogel.

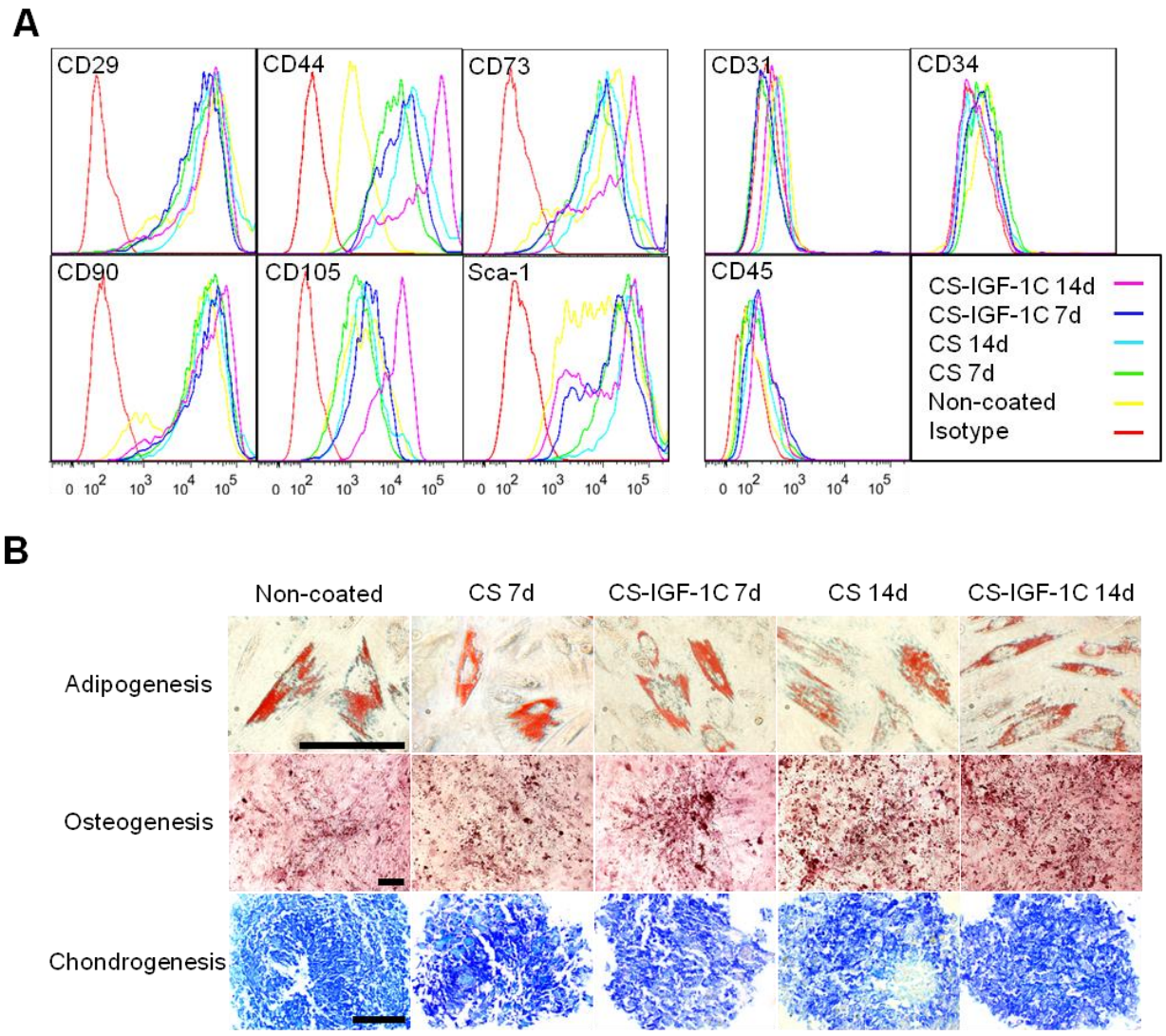

Supplemental Figure 4. Phenotypic and differentiation properties of ADSCs. (**A**) The phenotypic profiling of ADSCs was assessed by flow cytometry. ADSCs were cultured on non-coated, chitosan hydrogel coated, and CS-IGF-1C hydrogel coated plates during 2 weeks. (**B**) Induced differentiation of ADSCs towards cells of mesodermal lineage. ADSCs were pre-treated with chitosan or CS-IGF-1C hydrogel for 1 or 2 weeks before induction. Oil red O, alizarin red S, and toluidine blue staining were performed to evaluate their adipogenic, osteogenic, and chondrogenic differentiation, respectively. Scale bars, 100 μm. These experiments were performed in triplicate. CS, chitosan hydrogel.

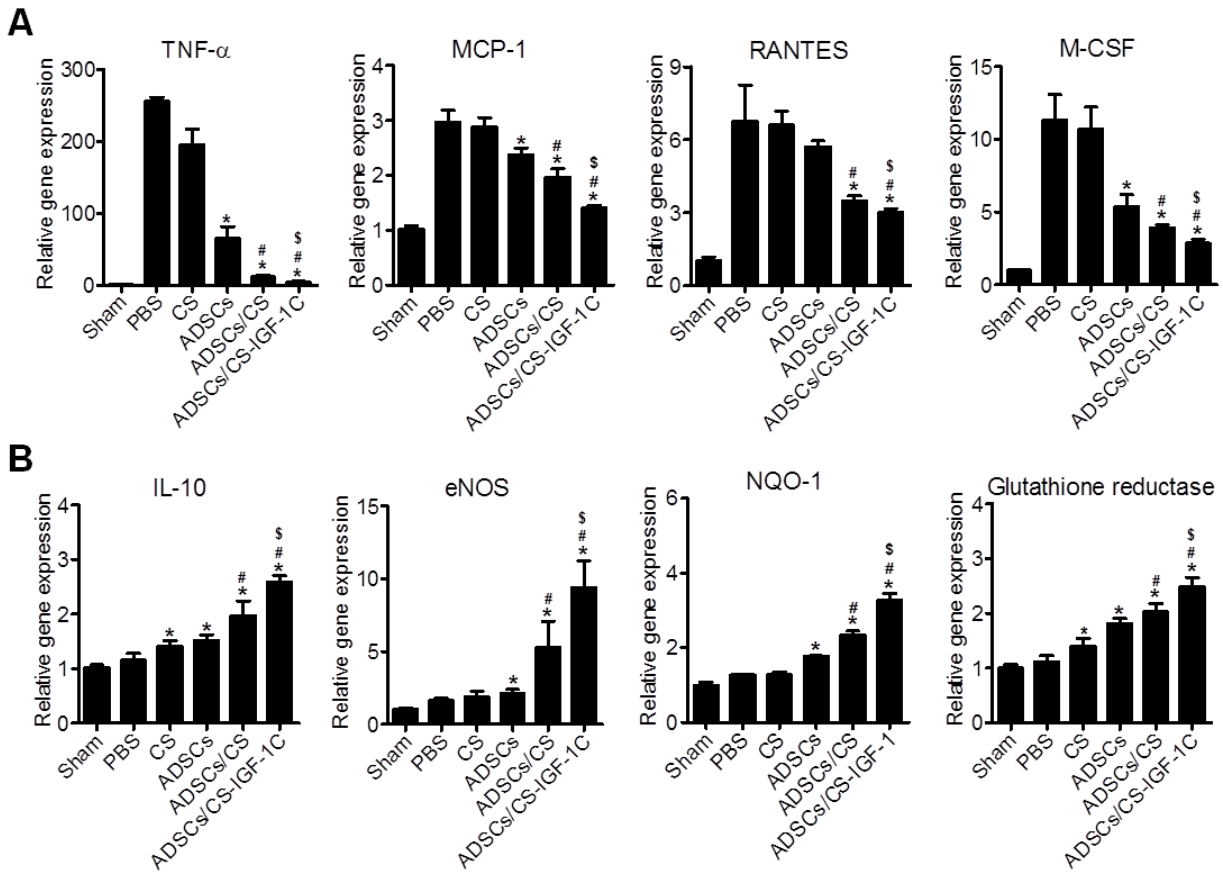

Supplemental Figure 5. CS-IGF-1C hydrogel increases anti-inflammatory actions of ADSCs in AKI. (**A**) Real-time RT-PCR analysis showing renal expression of pro-inflammatory genes 3 days after AKI. n=4. (**B**) Real-time RT-PCR analysis of renal expression of anti-inflammatory and anti-oxidative genes 3 days after AKI. n=4. Experiment was performed in triplicate. **P*<0.05 vs PBS, $^{\#}$*P*<0.05 vs ADSCs, $^{\$}$*P*<0.05 vs ADSCs/CS. Values are the mean±STD. CS, chitosan hydrogel; ADSCs/CS, ADSCs co-transplanted with chitosan hydrogel; ADSCs/CS-IGF-1C, ADSCs co-transplanted with CS-IGF-1C hydrogel.

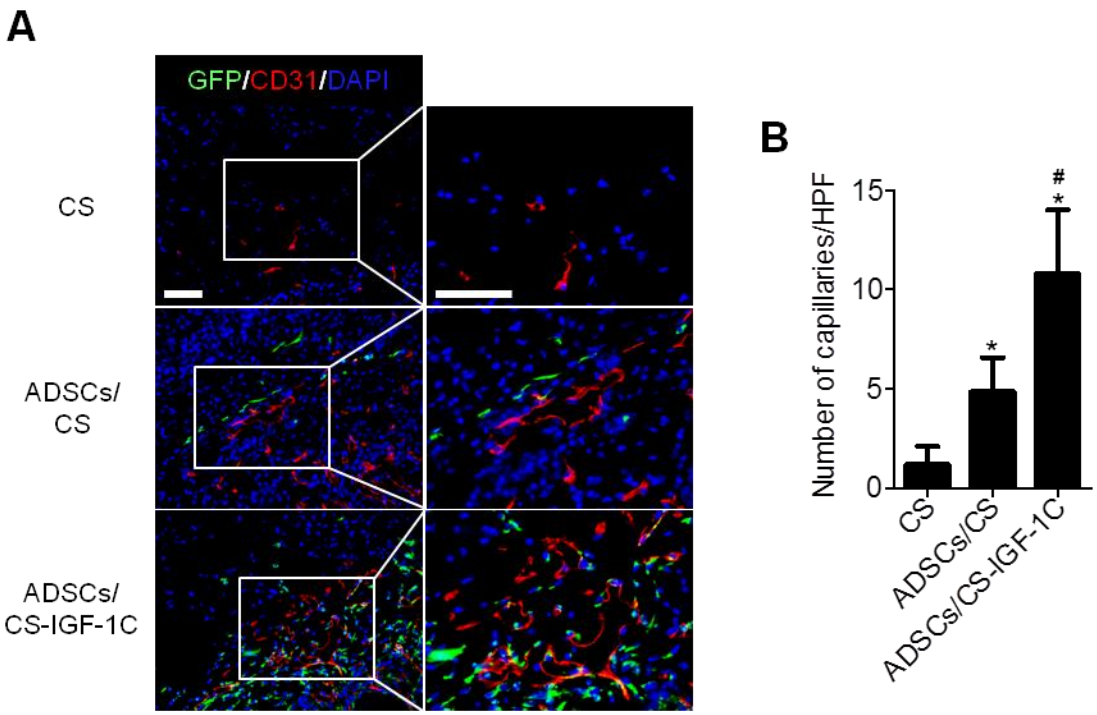

Supplemental Figure 6. CS-IGF-1C hydrogel promotes neovascularization in local microenvironment. (**A**) Representative images showing $CD31^+$ capillary (red) ingrowth within areas injected with CS, ADSCs/CS, and ADSCs/CS-IGF-1C at 3 days. (**B**) Quantification of capillary number. **P*<0.05 vs CS, $^{\#}P$<0.05 vs ADSCs/CS, n=5. Data in bar graphs are shown as mean ± SEM. Scale bars, 100 μm. HPF, high power field. CS, chitosan hydrogel; ADSCs/CS, ADSCs co-transplanted with chitosan hydrogel; ADSCs/CS-IGF-1C, ADSCs co-transplanted with CS-IGF-1C hydrogel.

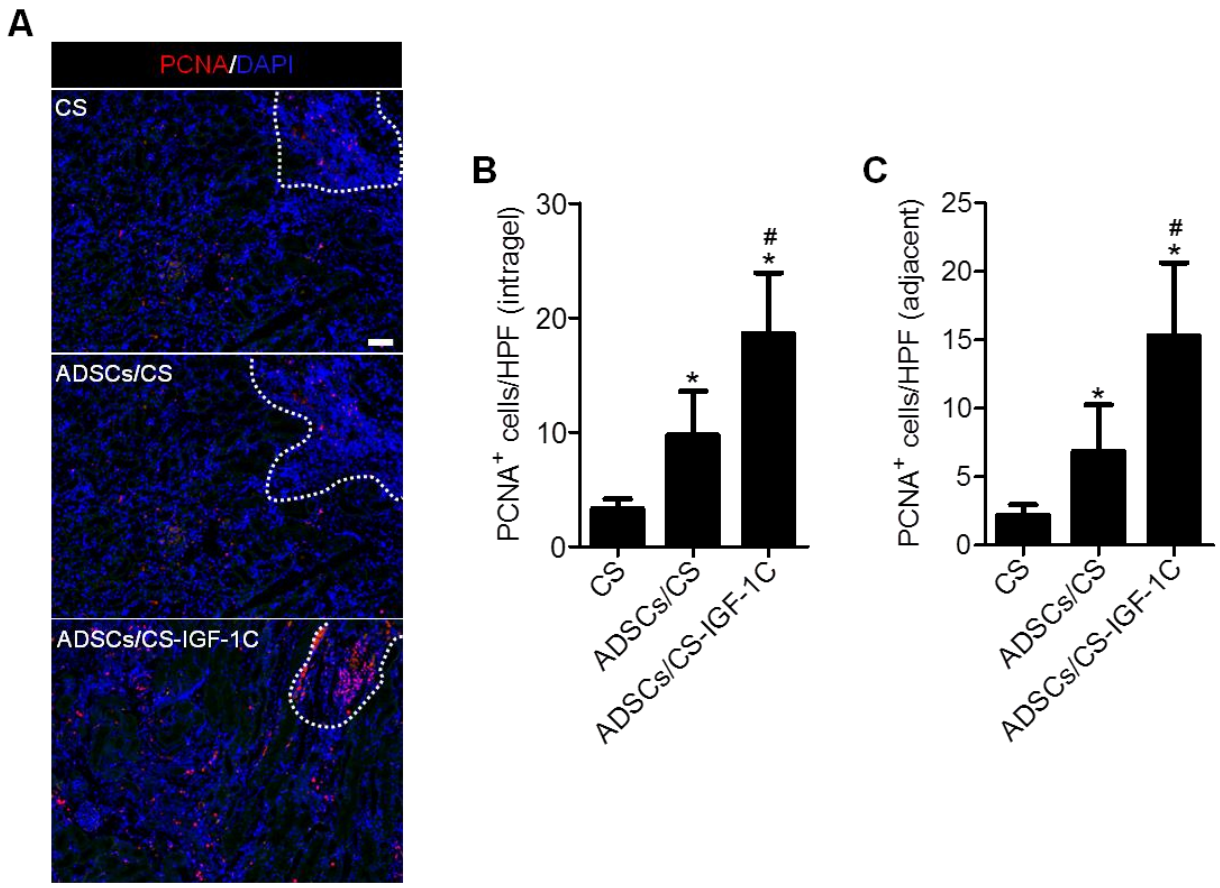

Supplemental Figure 7. CS-IGF-1C hydrogel enhances cell proliferation. (**A**) Representative images of PCNA-stained kidney sections showing proliferative cells (red) in intra-hydrogel and adjacent regions at 28 days (dashed lines indicate the graft region). (**B-C**) Quantification of proliferative cells within intra-hydrogel and adjacent regions. **P*<0.05 vs CS, $^{\#}$*P*<0.05 vs ADSCs/CS, n=5. Values are the mean±SEM. Scale bar, 50 μm. HPF, high power field. CS, chitosan hydrogel; ADSCs/CS, ADSCs co-transplanted with chitosan hydrogel; ADSCs/CS-IGF-1C, ADSCs co-transplanted with CS-IGF-1C hydrogel.

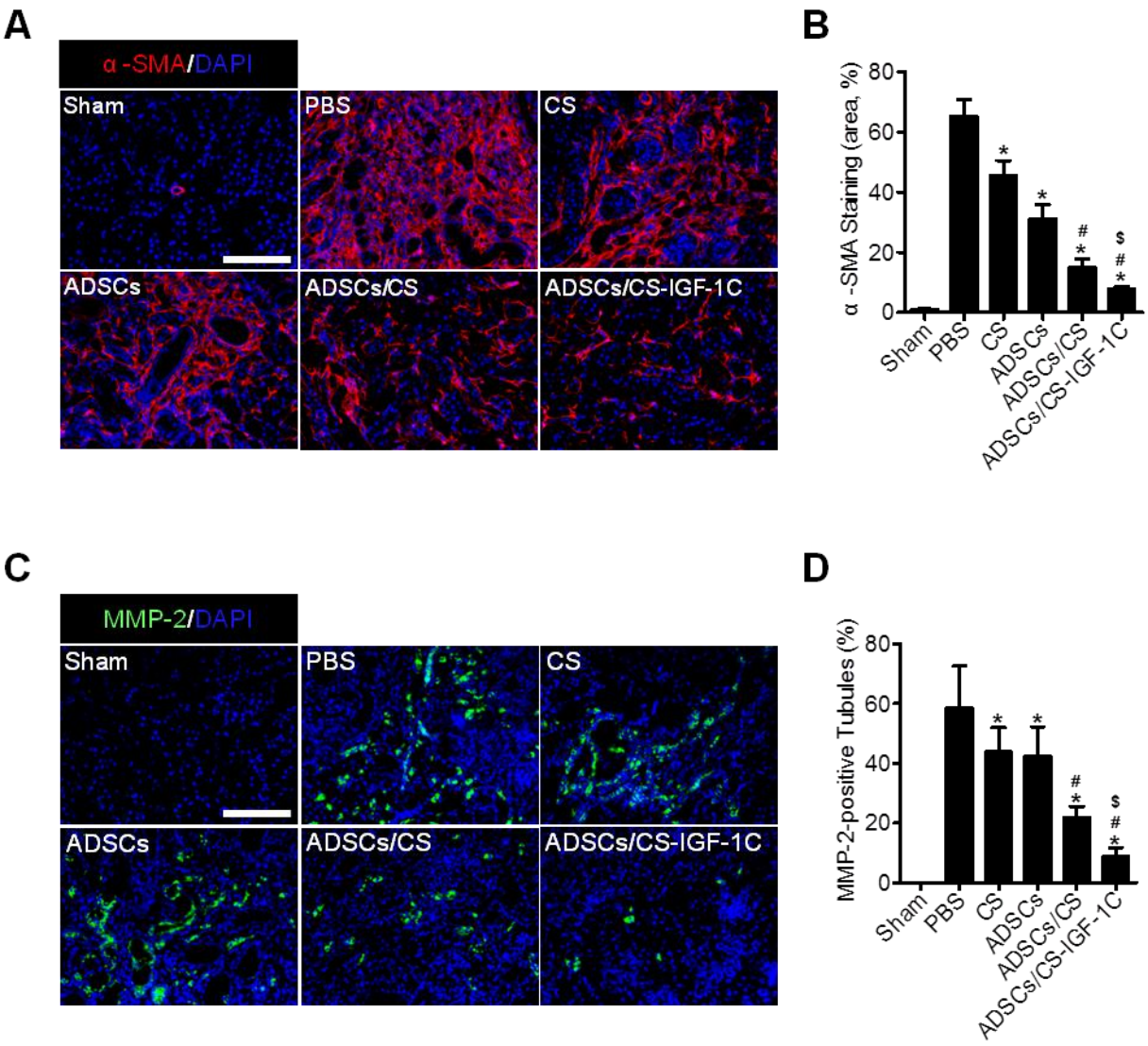

Supplemental Figure 8. Administration of ADSCs and CS-IGF-1C hydrogel decreases α-SMA and MMP-2 expression. (**A**) Representative images of kidney sections stained for alpha-SMA two months after injury. (**B**) Quantification of alpha-SMA staining. (**C**) Representative images of kidney sections stained for MMP-2 two months after AKI. (**D**) Quantification of MMP-2 staining. *P<0.05 vs PBS, $^{\#}P$ <0.05 vs ADSCs, $^{\$}P$<0.05 vs ADSCs/CS, n=5. Values are the mean±SEM. Scale bars, 100 μm. CS, chitosan hydrogel; ADSCs/CS, ADSCs co-transplanted with chitosan hydrogel; ADSCs/CS-IGF-1C, ADSCs co-transplanted with CS-IGF-1C hydrogel.

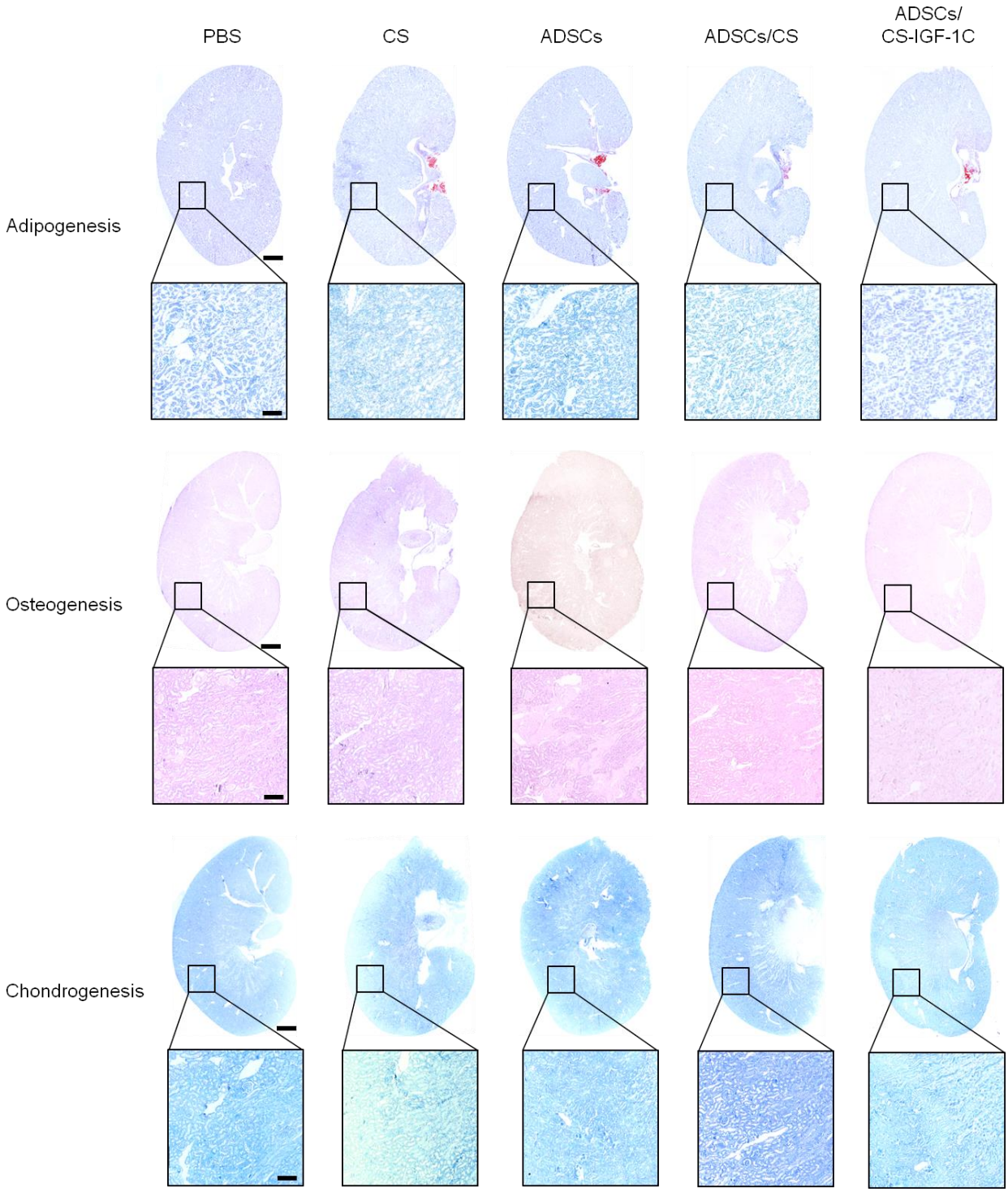

Supplemental Figure 9. **Long-term safety of transplantation of hydrogel and ADSCs.** Oil red O, alizarin red S, and toluidine blue staining were performed in 2-month kidney sections to evaluate adipogenic, osteogenic, and chondrogenic differentiation of ADSCs in different groups.

Note that renal pelvic adipose tissues can be positively stained by oil red O. Scale bars, 1000 μm in macro-view of kidney, 200 μm in the magnified images.

Reference

1. Kim, JH, Park, DJ, Yun, JC, Jung, MH, Yeo, HD, Kim, HJ, Kim, DW, Yang, JI, Lee, GW, Jeong, SH, Roh, GS, Chang, SH: Human adipose tissue-derived mesenchymal stem cells protect kidneys from cisplatin nephrotoxicity in rats. *Am J Physiol Renal Physiol*, 302**:** F1141-1150, 2012.
2. Cheng, S, Pollock, AS, Mahimkar, R, Olson, JL, Lovett, DH: Matrix metalloproteinase 2 and basement membrane integrity: a unifying mechanism for progressive renal injury. *Faseb J*, 20**:** 1898-1900, 2006.
3. Kunter, U, Rong, S, Boor, P, Eitner, F, Muller-Newen, G, Djuric, Z, van Roeyen, CR, Konieczny, A, Ostendorf, T, Villa, L, Milovanceva-Popovska, M, Kerjaschki, D, Floege, J: Mesenchymal stem cells prevent progressive experimental renal failure but maldifferentiate into glomerular adipocytes. *J Am Soc Nephrol*, 18**:** 1754-1764, 2007.